Absolute band-edge energies are over-emphasized in the design of photoelectrochemical materials

Aaron J. Kaufman[1], Adam C. Nielander[2], Gerald J. Meyer[3], Stephen Maldonado[4], Shane Ardo[5], Shannon W. Boettcher[1]*

[1]Department of Chemistry and the Oregon Center for Electrochemistry
University of Oregon, Eugene, Oregon

[2]SUNCAT Center for Interface Science and Catalysis,
SLAC National Accelerator Laboratory, Menlo Park, California

[3]Department of Chemistry, University of North Carolina at Chapel Hill,
Chapel Hill, North Carolina

[4]Department of Chemistry and Program in Applied Physics,
University of Michigan, Ann Arbor,

[5]Departments of Chemistry, Chemical & Biomolecular Engineering,
and Materials Science & Engineering, University of California Irvine

Corresponding Author e-mail: swb@uoregon.edu

The absolute band-edge potentials of semiconductors, i.e., the conduction-band minimum, valence-band maximum, and their relative positions to solution redox potentials, are often invoked as design principles for photoelectrochemical (PEC) devices, especially for particulate photocatalysts. Here we show that reliance on these criteria is not necessary and limits the exploration of materials that will advance the fields of photoelectrochemistry, photochemistry, and photocatalysis. We discuss how *i*) band-edge energies are not singular parameters and instead shift with pH, electrolyte type, and surface chemistry; *ii*) the free energy of electrons and holes in comparison to that of solution redox couples dictates overall reaction spontaneity and thus reactivity; and *iii*) favorable charge-transfer kinetics can occur even when the relevant electrolyte redox potential(s) appear 'outside' the bandgap, enabled by the inversion or accumulation of electronic charge at the semiconductor surface. This discussion informs design principles for photocatalyst systems engineering for both one-electron redox reactions as well as for more complex multi-electron transfer reactions (e.g, H_2 evolution, H_2O oxidation, CO_2 reduction).

Suppose one desires to identify a semiconductor material that can photo-reduce a species with a formal reduction potential, $\mathcal{E}^{o'}$. Such a reduction could be a one-electron transfer for application in organic synthesis, environmental remediation, solar-energy conversion, or kinetically complex multi-electron transfer as in the reduction of H_2O or H^+ to H_2 fuel. A typical starting point would be to consult a photoelectrochemistry review article for band-edge positions of semiconducting materials versus the vacuum energy level and/or the standard hydrogen electrode (SHE) energy level, typically in an aqueous electrolyte.[1-4] With knowledge that band-gap photoexcitation creates electron-hole pairs that relax/thermalize to the band edges before interfacial electron transfer occurs, an inspection of the tabulated conduction band edge energy, $\mathbf{E}_c$ value, relative to the $-q\mathcal{E}^{o'}$ would appear to predict whether a given semiconductor was appropriate for the desired reactivity. One might also conclude that interfacial electron transfer from the semiconductor into solution would not occur at all if $-q\mathcal{E}^{o'} > \mathbf{E}_c$, i.e. if the reduction potential lies above the conduction band energy. *These ideas are flawed.* A reduction potential that falls outside the semiconductor bandgap may impact the current-voltage behavior and applied-voltage-dependent interfacial kinetics, but does not in fact preclude facile electron transfer.

Tabulated band-edge positions are poor indicators of interfacial redox chemistry because *i*) they are not singular parameters, *ii*) are sensitive to the chemical environment and surface chemistry, and *iii*) are modulated in energy by interface electrostatics. The free energies of the non-equilibrium electronic charge carriers (e.g. hole and electron quasi-Fermi levels) within the semiconductor, at steady state and under illumination, determines the ability to drive overall reactions and perform chemical work.[5] The degree to which the quasi-Fermi levels split under illumination, in turn depends on the kinetics of charge transfer, i.e. the surfaces or interfaces acting as charge-carrier selective contacts, *not on the absolute band-edge energies in any simple way*. We discuss the origins of the common misconception that absolute band edges are most-critical, and illustrate underlying design principles for improved materials design, operative charge-separation/collection mechanisms, and materials-stabilization strategies at semiconductor-electrolyte interfaces. Symbols used in this contribution are defined in Table 1.

Table 1 | Symbol definitions			
term	***symbol***	***unit***	***brief definition***
elementary charge	q	C	magnitude of charge on a single electron, (F/N_A)
stoichiometric number	ν_i	unitless	number of species i in balanced equation
signed charge number	z_i	unitless	signed charge number of species i (e.g., +2, +1, 0, -1, -2)
Avogadro's constant	N_A	mol^{-1}	number of entities in one mole of a given substance
Faraday constant	F	$C{\cdot}mol^{-1}$	magnitude of charge per mole of protons
electron-transfer rate constant	$k_{rxn\#,et}$, $k'_{rxn\#,et}$	$cm^4{\cdot}s^{-1}$	rate constant for a second order heterogeneous surface reaction; the prime indicates the reverse reaction
hole-transfer rate constant	$k_{rxn\#,ht}$, $k'_{rxn\#,ht}$	$cm^4{\cdot}s^{-1}$	as above, except for holes
electron concentration	n, $n_{rxn\#,s}$, $n^{eq}_{rxn\#,s}$	cm^{-3}	concentration of electrons in the conduction band (n), the surface concentration is with a subscript *s*, and *eq* indicates the equilibrium value
hole concentration	p, $p_{rxn\#,s}$, $p^{eq}_{rxn\#,s}$	cm^{-3}	as above, except for valence-band holes (p)
activity	a_i^α	unitless	activity of species i in phase α defined by $a_i^\alpha = \gamma_i^\alpha C_i^\alpha / C_i^{0,\alpha}$ where, γ_i^α is the activity coefficient, C_i^α is the concentration and $C_i^{0,\alpha}$ is a reference concentration, usually taken to be 1 M for soluble species.
electrostatic potential	ϕ	V	electric work needed to move a test charge to a specific point in space from a reference point (often at infinite distance) divided by the value of the charge
reduction potential	$\mathcal{E}$	V	free-energy change divided by the electron charge associated with moving an electron (and any associated ion/solvent movement/rearrangement) from a reference state (often a reference electrode) into the bulk of a solution via a redox reaction
formal reduction potential	$\mathcal{E}^{o'}$	V	measured potential of a reduction reaction with concentration of each species at standard-state values
effective conduction/valence band density of states	N_C or N_V	cm^{-3}	the number per volume of thermally accessible electron or hole states at $\mathbf{E}_c$ or $\mathbf{E}_v$, respectively
charge density	ρ	$C{\cdot}cm^{-3}$	the amount of electric charge per unit volume
Debye length	λ	cm	a characteristic length over which mobile charge carriers screen an electric field, which decreases with mobile carrier density
depletion width	w	cm	length over which mobile carriers are depleted at a doped semiconductor surface or junction
donor or acceptor density	N_D or N_A	cm^{-3}	number density of electrons or holes donated to the conduction or valence band by impurity atoms
vacuum energy/level	$\mathbf{E}_{vac}$	eV	energy of a free stationary electron outside of a material, typically defined to be 0
conduction / valence band edge	$\mathbf{E}_c$, $\mathbf{E}_v$	eV	energies analogous to LUMO and HOMO for semiconductor solids. Often referenced to vacuum level
band gap	$\mathbf{E}_g$	eV	energy separation between $\mathbf{E}_c$ and $\mathbf{E}_v$
electrochemical potential	$\bar{\mu}_i^\alpha$	$J{\cdot}mol^{-1}$	partial-molar Gibbs free energy of a given species i in phase α, which defines criteria for equilibrium
chemical potential	μ_i^α	$J{\cdot}mol^{-1}$	partial-molar Gibbs free energy, ignoring long-range electrostatic contributions
Fermi level	E_{fn} , E_{fp}, E_f	eV	electrochemical potential of electrons in a phase α, $\bar{\mu}_e^\alpha$; subscripts *p* and *n* refer to only considering carriers in the valence or conduction band, respectively.
Gibbs free energy	G	J	thermodynamic potential used to calculate the maximum amount of non-pressure-volume work that may be performed at constant temperature and pressure
open-circuit voltage	V_{oc}	V	the difference in electron electrochemical potential (divided by charge) between two contacts with no external current flow

First consider a semiconductor without dopants and without interfacial electric fields at equilibrium (i.e., the so-called flat-band condition). With generality to molecular, particulate, and bulk semiconductor photoabsorbers, we can write, for a pair of redox reactions (either outer-sphere one-electron reactions or multi-step electron-transfer reactions), the equilibrium expressions including both electrons and holes and species *O* (oxidized) and *R* (reduced), with the specific charge not included for simplicity of notation:

$$\text{Reaction 1: } \nu_1 e_{cb}^- + O_1 \underset{k'_{1,et}}{\overset{k_{1,et}}{\rightleftharpoons}} R_1, \quad \nu_1 h_{vb}^+ + R_1 \underset{k'_{1,ht}}{\overset{k_{1,ht}}{\rightleftharpoons}} O_1 \tag{1}$$

$$\text{Reaction 2: } \nu_2 e_{cb}^- + O_2 \underset{k'_{2,et}}{\overset{k_{2,et}}{\rightleftharpoons}} R_2, \quad \nu_2 h_{vb}^+ + R_2 \underset{k'_{2,ht}}{\overset{k_{2,ht}}{\rightleftharpoons}} O_2 \tag{2}$$

Marcus theory shows how the standard electron-transfer rate constant can be cast for an outer-sphere redox reaction (i.e. where electron transfer is *across* the double layer) in terms of the energy difference between the band-edge and redox energy[6,7]. While in some ideal cases Marcus theory describes the kinetics of electron transfer from a SC to molecular acceptors[8,9], photochemical fuel-forming reactions don't generally proceed as purely outer-sphere reactions, but instead involve catalyst species and mechanistic steps with inner-sphere intermediates (i.e. that may interact in the strong-coupling limit).[10] Further, band-edge positions are generally unknown under the experimental conditions of interest as they are not singular parameters. Ab initio calculations can provide a guide, but are limited in that they assume an atomic-scale structure and termination of the active surface and interface solvent / double-layer structure that is typically experimentally unknown. Predicting rate constants for practically relevant photoelectrochemical processes thus remains a major challenge.

The free energy of charge carriers in the semiconductor is described by their electrochemical potential $\bar{\mu}_i^{\alpha}$. Generally, (assuming thermal equilibrium) for species *i* in phase α:

$$\bar{\mu}_i^{\alpha} = \mu_i^{\alpha} + z_i F \phi^{\alpha} = \left(\mu_i^{0\alpha} + RT \ln a_i^{\alpha}\right) + z_i F \phi^{\alpha} = \left(\frac{\partial G}{\partial \nu_i}\right)_{T,P,\nu_{j\neq i}} \tag{3}$$

Under illumination, one can separate the electrochemical potential of conduction-band electrons from valence-band holes. In semiconductor physics, these quantities are termed the electron and hole quasi-Fermi levels (E_{fn} and E_{fp}). Although quasi-Fermi levels are understood for populations of electronic charge carriers, the concept applies in the ergodic limit to small or individual species[11]. For example, if a semiconductor particle is sufficiently small that there are few excited carriers, the *time-averaged behavior* is equivalent to the ensemble average across many particles and energies can be described by the quasi-Fermi-level concept. Regardless of the band-edge position at the flat-band condition, the quasi-electrochemical potential of conduction-band electrons and valence-band holes in the photoabsorber, $\bar{\mu}_n^{\mathrm{absr}}$ and $\bar{\mu}_p^{\mathrm{absr}}$, respectively, will tend toward equilibrium, transferring charge via Eqns. (1) and (2), or via recombination of electrons and holes at the surface and within the bulk of the photoabsorber. To drive an overall "uphill" ($\Delta G_{\mathrm{rxn}} > 0$) chemical reaction with light, the quasi-Fermi-level splitting (E_{fn} - E_{fp}) must be larger in magnitude than ΔG_{rxn} under the steady-state reaction conditions (and relevant species activities at the surface). Differences between E_{fn} and E_{fp} beyond this minimum energy value are needed due to associated kinetic (catalysis) and mass-transport energy losses.

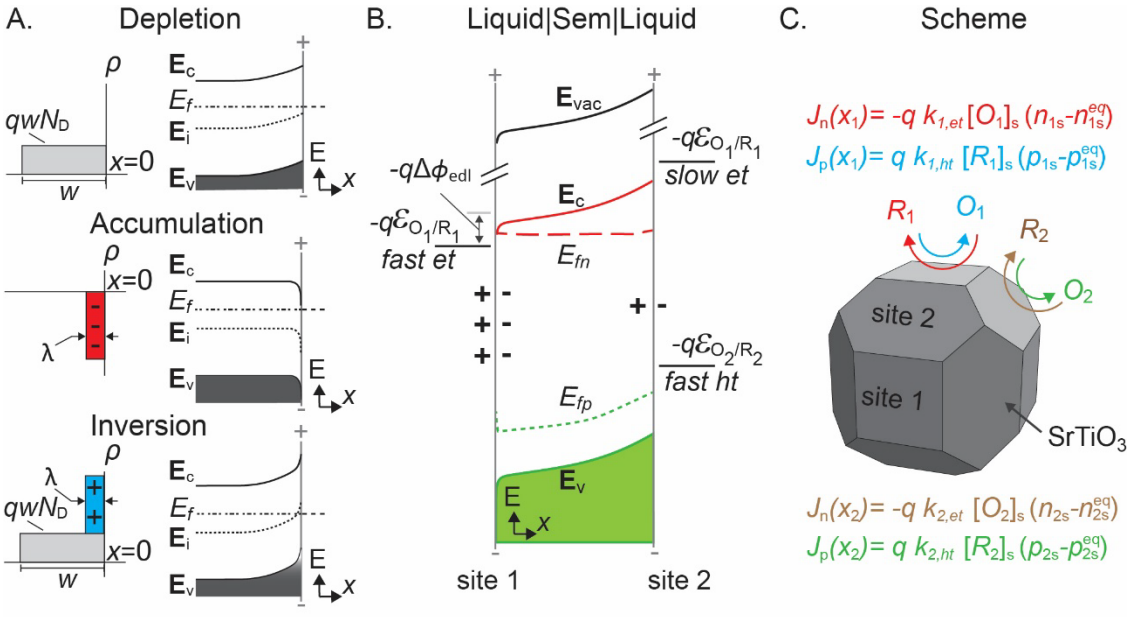

Figure 1 |Interface energies and reactions. (a) Excess charge-carrier-density plots (left) and band diagrams (right) of an n-type semiconductor in depletion, accumulation, and inversion due to equilibration with a contacting phase (e.g., redox species). **(b)** Depleted photoabsorber particle (right contact) driving "misaligned" half reactions under illumination, (simulated 1D COMSOL Multiphysics model, N_D = 10^{14} cm^{-3}, length 1 µm, and disparate *et* and *ht* rates at the electron- and hole-selective contacts, respectively). Accumulated surface electrons (left contact) "pull up" the photoabsorber energy levels relative to $q\mathcal{E}_{O_1/R_1}$ by an electrostatic potential energy $q\Delta\phi_{edl}$, allowing photoexcited electrons to drive a reduction reaction on the semiconductor (sem) surface whose energy is out of the bandgap. **(c)** Possible facet-dependent oxidation or reduction kinetics and rate equations which quantify charge-carrier selectivity, as discussed in the text.

Semiconductor|liquid junctions. Next consider a wide-band-gap ($\mathbf{E}_g$ ~3-4 eV) semiconductor particle with conduction band energy (or equivalently potential, which is energy per charge on the relevant reference scale) "not high enough to drive HER" (i.e., not reducing enough to drive H^+/H_2) but a valence band substantially below (i.e. more oxidizing) than the reversible oxygen reduction potential (**Figure 1**). Under illumination, a small photoexcited carrier concentration (n' and p') is needed to produce the minimum thermodynamically required difference between $\bar{\mu}_n^{absr}$ and $-\bar{\mu}_p^{absr}$ to drive water splitting because of the low equilibrium concentration of holes and electrons (n^{eq} and p^{eq}) in a large-gap semiconductor. The total free energy available to drive chemical reactions is given by the difference in electron and hole quasi-Fermi levels (or equivalent electrochemical potentials as cast in **Eqn. 3**).

$$E_{fn} - E_{fp} = \mathbf{E}_g + RT\ln\frac{n'p'}{N_C N_V} = RT\ln\frac{n'p'}{{n_i}^2} > \Delta G_{rxn}\ (+\Delta G_{losses}) \tag{4}$$

The term n_i is the intrinsic carrier concentration. Notice that **Eqn. 4** does not include variables associated with the kinetics of the electron-transfer reactions or the absolute band-edge positions. How can both electrons and holes transfer, if the conduction band edge energy isn't "high enough" to drive the reaction? Consider the following *qualitative* picture. The kinetics of hole transfer from semiconductor to solution

species initially will be fast as the valence band holes are quite oxidizing, while electrons transfer slowly. This will lead to build-up of negative electron charge on/in the semiconductor, which is equivalent to an applied negative bias that shifts the quasi-Fermi level of electrons, and eventually the band edges, higher and thus increases the reducing power of the photoexcited electrons. *This process will occur until the rates of both hole and electron transfer are equal (at steady state).* If the semiconductor particle is already doped *n*-type, like most metal oxides used in water splitting[12-15], this negative charging under photoexcitation is termed "majority carrier accumulation". The same phenomena can occur with the addition of excess minority carriers, which is called "inversion". The excess mobile carriers reside close to the surface of the semiconductor, typically within the first few atomic layers as required by Gauss's Law (**Figure 1a**). Critically, this analysis assumes that there is no chemical change (e.g., cation intercalation/deintercalation, changing surface termination, surface oxidation formation, etc.) that modifies the surface electrochemical chemical potential without requiring the development of excess space charge — such processes can also play an important role in dictating interfacial energetics[16-18].

Experimental data supports the qualitative picture above[19-22]. Grimm et al. showed systematic control of the interface photovoltage in H- and CH_3-terminated crystalline *p*-Si and *n*-Si photoelectrodes near the bulk-recombination limit, governed by the reversible potential of the solution redox couple (**Figure 2a**)[22]. These surfaces have low defect densities, with nearly every Si surface atom chemically terminated. If the redox potential of the solution "was outside the band gap" of the Si (i.e. under flat-band conditions), the interface was driven into either *i*) inversion (minority carrier concentration at the surface exceeds the majority carrier concentration in the semiconductor bulk), creating the equivalent of a buried junction leading to high photovoltages, or *ii*) accumulation (excess majority carriers at the surface), leading to an ohmic contact between the solution and semiconductor[23].

While the 'regenerative photoelectrochemical cell' architecture' used by Grimm et al. has only one electrochemically active semiconductor interface, the demonstration of large bulk-recombination-limited photovoltages with effective solution potentials outside the absolute-energy limits of the Si bandgap are conceptually the same as the picture described for the hypothetical wide-bandgap semiconductor described above. The difference between the H- and CH_3-terminated surface leads to a systematic shift in the band-edge positions of ~0.4 V, highlighting that band edges can be significantly modified by surface chemistry without changes to the maximum interface photovoltage or the ability to drive any given redox reaction[24]. *Regardless of the relative positions of the solution reduction potential/energy and the band-edge energy positions, photoexcited carriers are able in all cases to drive the photochemical reactions.* In fact, the highest photovoltages were observed in the case of a *p*-Si photoelectrode in contact with a redox couple (labeled **A** in **Figure 2a**), dimethylcobaltocene, whose reduction potential near -1 V vs SCE is much more negative than the conduction band edge (at flat band) for Si at only about -0.6 V versus SCE[25,26]. Hence, the absolute conduction band energy/potential value is irrelevant for determining which reductions *p*-Si can drive. Evidence for inversion has been reported at photoelectrochemical interfaces via near-surface-channel conductance measurements[27], photo-capacitance[28], and infrared spectroscopy[29].

In the absence of other observations, the data in **Figure 2a** could also be explained by densities of surface states that prevent larger degrees of band-banding and high photovoltages (i.e. surface-state induced Fermi-level pinning)[30,31]. However, near-surface-channel conductance measurements on some of the systems argue against this possibility[27]. Nevertheless, when large densities of surface states do cause Fermi-level pinning, the resultant photoelectrode behavior is like that of a buried junction or a

photoelectrode in inversion – the photovoltage is independent of the redox potential of the solution and the absolute band-edge energies remain irrelevant with regard to which reactions can be driven.

The data in **Figure 2a** is the result of measurements that spanned the semiconductor operating in either accumulation, depletion, or inversion conditions. At semiconductor/liquid junctions, the simplest electrostatic model consists of two "capacitors", one representing the charge stored in the semiconductor space-charge region (C_{sem}) and the other the Helmholtz or double layer (C_{edl}). More-extensive models including the diffuse layer, accounting for interfacial surface states, and other corrections can also be used[3], but are not needed to illustrate accumulation, depletion, and inversion conditions. The absolute electrostatic potential drops ($\Delta\phi$) across the space-charge region and double layer are inversely related to their relative capacitances by the conservation of charge (**Figure 2b**), where equilibration of the surface electrochemical potential sets the degree of band bending and therefore the potential dropped in the semiconductor ($\Delta\phi_{\mathrm{sem}}$).

$$\frac{\Delta\phi_{\mathrm{sem}}}{\Delta\phi_{\mathrm{edl}}} = \frac{C_{\mathrm{edl}}}{C_{\mathrm{sem}}} \tag{5}$$

The surface charge and C_{sem} depend on the applied potential in a manner that can be calculated from carrier statistics and Poisson's equation[26], but the key point is that the magnitudes of the potential drops in each region depend on both C_{sem} and C_{edl}. The smaller quantity between C_{sem} and C_{edl} requires that $\Delta\phi$ is larger in that region. Simply, the smaller capacitance reflects where the electrostatic potential change is larger. Plots of the measured capacitance as a function of electrode potential thus may readily illustrate when accumulation or depletion conditions are operative, but such data is rarely reported presumably due to the presence of surface states[32].

As a semiconductor electrode is biased into accumulation, the experimentally measured capacitance, C_{exp}, increases and saturates to the value of C_{edl}. In this condition, $\Delta\phi_{\mathrm{edl}}$ is larger than $\Delta\phi_{\mathrm{sem}}$. That is, applying a bias to a semiconductor electrode in accumulation does not significantly move the (quasi-)Fermi levels relative to the band-edges. Instead, the applied bias primarily shifts the band edges *relative* to a reference point in solution. Through Eqn. 5, the quantity of charge from majority carriers (i.e. $\Delta\phi_{\mathrm{sem}} \cdot C_{\mathrm{sem}}$) accumulated at the semiconductor surface must be counter-balanced exactly by the charge from ions in solution (i.e. $\Delta\phi_{\mathrm{edl}} \cdot C_{\mathrm{edl}}$) gathered at the interface. Physically, the availability of ions from solution to this location is limiting because the abundance of majority carriers from within the semiconductor at the surface is large in accumulation, i.e. $C_{\mathrm{exp}} \rightarrow C_{\mathrm{edl}}$.

In depletion, the opposite is true. $C_{\mathrm{exp}} \rightarrow C_{\mathrm{sem}}$ because the total charge from majority carriers in the semiconductor space charge is much smaller than available ions in solution that could move to the interface. Correspondingly, $\Delta\phi_{\mathrm{sem}}$ is significantly larger than $\Delta\phi_{\mathrm{edl}}$ in depletion. This statement is equivalent to stating that the applied bias moves the (quasi-)Fermi levels relative to a reference point in solution, but the band-edge values are largely unchanged relative to that same reference point.

In accumulation, the interpretation of $\Delta\phi_{\mathrm{sem}}$ is straightforward. C_{sem} is effectively time/frequency-independent because equilibration of majority carriers from the bulk to the interface is fast on the relevant timescale of the impedance measurement. In inversion, the interpretation of $\Delta\phi_{\mathrm{sem}}$ is more nuanced. C_{sem} can have a measurable time dependence as supply of minority carriers at the surface depends on an interplay between the rate of thermal generation, drift, losses from recombination, and consumption from interfacial processes. Accordingly, the measured capacitance-potential profile in

inversion is a function of the frequency of measurement/observation (**Figure 2b** dotted versus solid line) and is strongly influenced by the operative kinetics of minority carrier generation, transport, trapping, and transfer[33]. This point is why Mott-Schottky plots of impedance often remain linear in inversion at potentials well past the band edge and can make the increase in measured capacitance due to inversion difficult to observe[32,34-40].

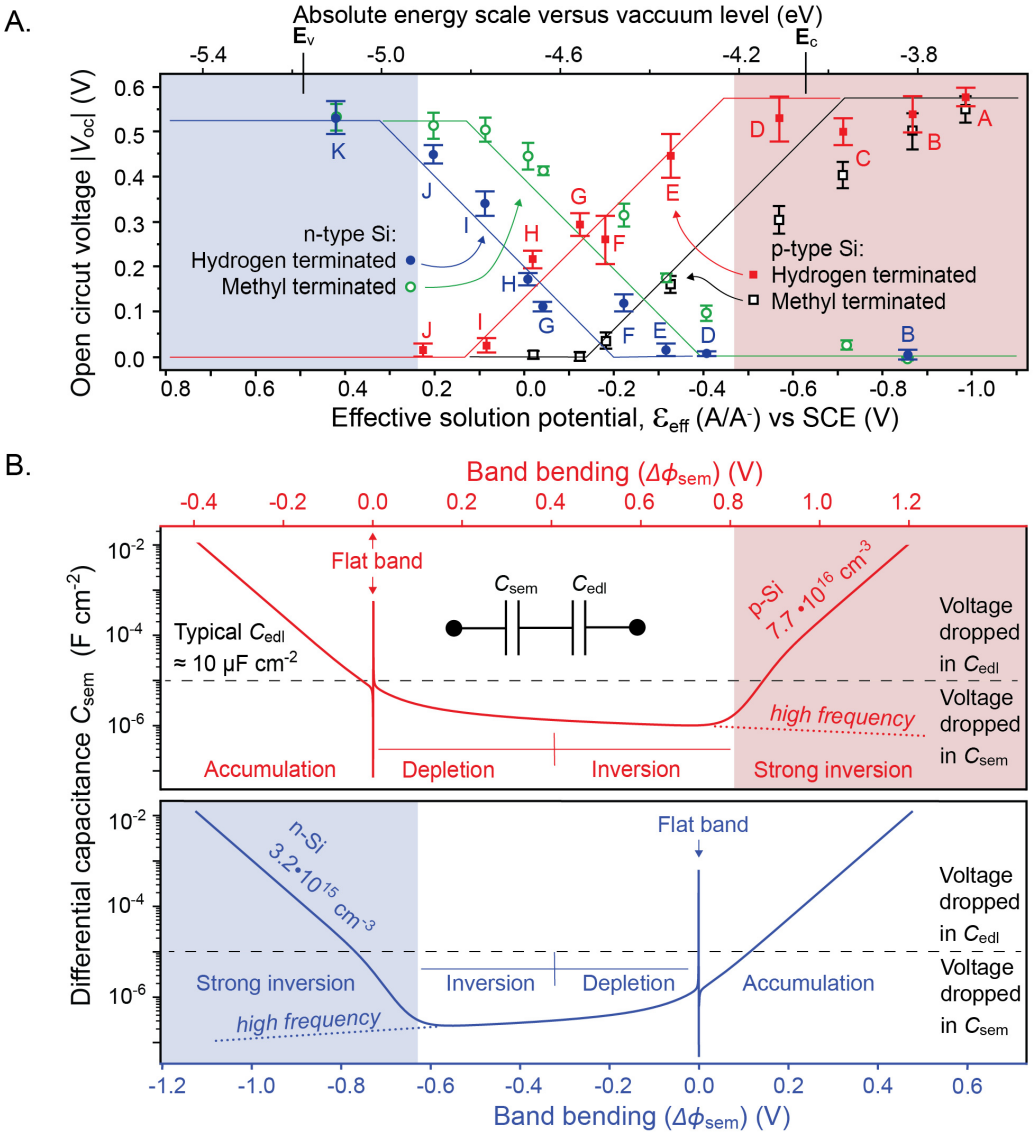

Figure 2 | Accumulation, depletion, and inversion at photochemical junctions. (A) The V_{oc} for *n*-type and *p*-type H- and CH_3-terminated Si as a function of the reducing power of the redox species in the electrolyte $\mathcal{E}_{\mathrm{eff}}(A/A^{-})$ (data from Ref. [22]) that is aligned with the absolute energy scale and the differential capacitances in Panel b. Here, the V_{oc} was directly measured from the semiconductor against a Pt electrode poised at the Nernstian potential of the solution, $\mathcal{E}(A/A^{-})$ and plotted against an effective solution potential, $\mathcal{E}_{\mathrm{eff}}(A/A^{-})$ normalizing the minority-carrier acceptor concentration to 10 mM. The blue and red highlighted regions correspond to strong inversion for *n*-type Si ($3{\cdot}10^{15}$ cm^{-3}) and *p*-type Si ($8{\cdot}10^{16}$ cm^{-3}), respectively. (B) The semiconductor differential capacitance (C_{sem}) is from the space-charge density,

adapted from Sze, as a function of the band bending ($\Delta\phi_{sem}$)[26]. The vertical asymptotes correspond to the flat-band potentials. The C_{sem} were plotted for *n*-type Si (blue) and *p*-type Si (red) at 295 K with the same dopant density as used by Grimm[22]. A double-layer capacitance C_{edl} of 10 μF cm^{-2} is shown as an approximate reference for relative voltage drops ($\Delta\phi_{edl}$, $\Delta\phi_{sem}$). The expected high-frequency dark response in the inversion region is shown by a dotted line when the minority carrier generation rate at the surface is slow.

Nanoscopic and molecular systems. In a bulk semiconductor the number of band-edge states is large compared to the number of carriers at the surface. Thus, the chemical potential at the surface does not change with the build-up of charge (i.e., the activity term a_i^{α} for charge carriers in Eqn. 3 becomes large and unaffected by further change in carrier density at the surface as in a polarized metal electrode).

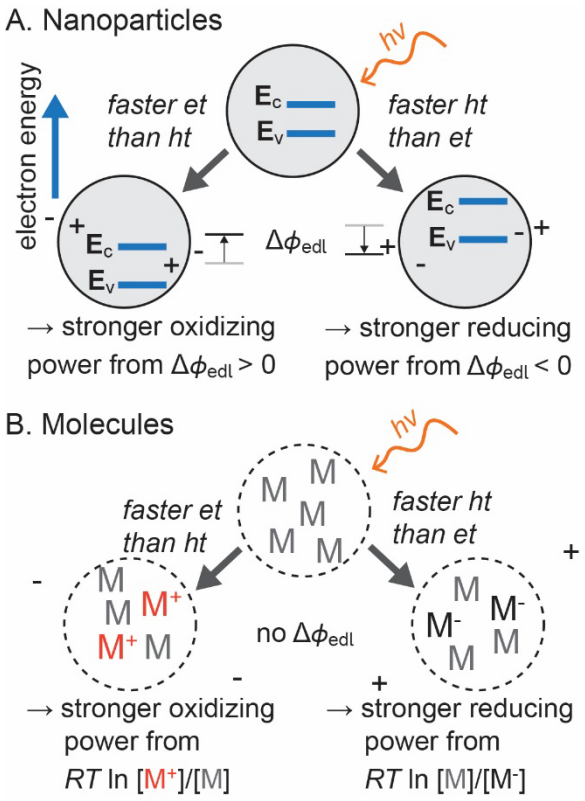

Figure 3 | Effects of photochemical charge accumulation in nanoscopic and molecular systems. (A) Due to kinetic limitations of either electron transfer (*et*) or hole transfer (*ht*), nanoparticles can accumulate either multiple electrons or holes, respectively, at steady state. This process leads to changes in the reducing or oxidizing power of these carriers associated with changes in electrostatic potential profiles. (B) Molecular energy levels are typically well-spaced leading to changes in reducing or oxidizing power of the ensemble via effects described to first order by the Nernst equation and thus are more limited in range.

Nanoscopic and molecular systems have similar behavior (**Figure 3**), but there are differences. Semiconductor nanoparticles are typically (practically) undoped. Yet under illumination they can accumulate electrons or holes at steady state. In general, the rates of photochemical *et* and *ht* are not

initially identical, *but they must be at steady state where the time derivatives of all concentrations are zero*, leading to an electrostatic potential developing across the nanoparticle/solution interface. This $\Delta\phi$ will move the energies of the band edges relative to the solution reduction potential (or energy) for the reasons stated above. The steady-state electron and hole concentrations will be defined by the reactant and product concentrations, charge-transfer rate constants, and relevant generation/recombination mechanisms and rates.

For soluble molecular systems (**M**) the initial rates of *et* and *ht* will also not be identical, and thus molecular systems can also accumulate $\mathbf{M}^-$ or $\mathbf{M}^+$ at steady state (representing an additional negative or positive charge on **M**, which may also initially charged). This process shifts the Nernst potential of the redox solution through a change in activities; $\mathcal{E}_{M^+/M} = \mathcal{E}^{\circ}_{M^+/M} + \frac{RT}{nF}\ln\frac{a_{M^+}}{a_{\mathrm{M}}}$ and $\mathcal{E}_{M/M^-} = \mathcal{E}^{\circ}_{M/M^-} + \frac{RT}{nF}\ln\frac{a_M}{a_{M^-}}$. In a molecule, the electronic states are usually widely spaced in energy and thus it is not generally possible to build-up charge at one energy level (such as is possible at the band edges in a semiconductor). Hence there is no mechanism to smoothly vary the electric potential term via a process analogous to accumulation or inversion in a semiconductor; instead, changes in chemical potential dominate contributions to changes in free energy under photoexcitation. As such, the only mechanism to change the oxidation or reduction strength of a specific molecular chromophore is by changing the activity of the oxidized or reduced species (or by changing the solvent or electrolyte).

The importance of charge-transfer kinetics and interface/contact selectivity. If band-edge energy positions (at flat band) don't matter much for semiconductor photoelectrochemistry, what does? *Charge-transfer kinetics and interface charge-carrier selectivity.* Consider a photoelectrode that has been fabricated to have a buried n^+p junction, such as Pt/n^+p-Si, and used as an efficient photocathode for photoelectrochemical H_2 production (**Figure 4**)[4]. The n^+p junction is selective for the collection of photoexcited electrons over holes because of the higher conductivity for electrons compared to holes in the n^+ region[41]. Pt makes an ohmic, unselective contact to the n^+-Si surface (emitter) layer, but that is inconsequential to the system behavior because the n^+ Si layer is very thin and absorbs little light; photocurrent is dominated by electron–hole pairs that separate at the n^+p junction prior to reaching the Pt/n^+-Si junction. The n^+p junction here is functionally equivalent to the case of strong inversion. Such an interface can be contrasted with Pt/*p*-Si, which is not very selective for electrons over holes because the relative lack of interfacial band bending leads to significant surface-hole concentrations and hole conductivity. In all these cases, the absolute band edges of the semiconductor are irrelevant to the ability of the photoelectrode to drive an efficient faradaic reaction.

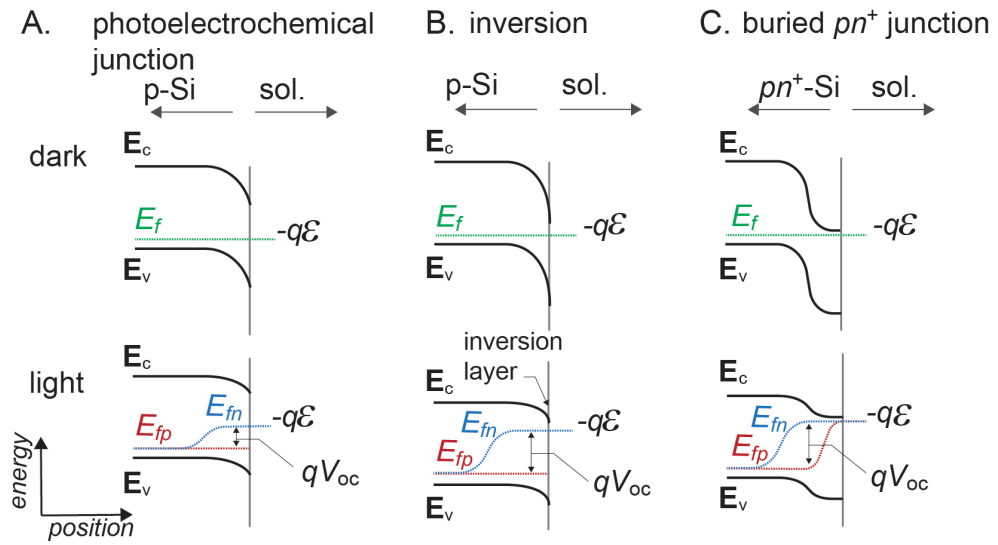

Figure 4 | Example band diagrams in the dark and under illumination of a photoelectrochemical junction (a) in typical depletion, (b) with an inversion layer (c) with a buried *pn*⁺ junction. Notice both the inversion layer and the buried junction can equivalently shift $\mathbf{E_c}$ and $\mathbf{E_v}$ relative to the solution redox potential, as in this example, due to an additional electric potential drop across the EDL.

In a simple model including carrier generation and interfacial-charge transfer, Roe et. al. derived the limits on the $V_{\mathrm{oc}} \leq (E_{fn} - E_{fp})/q$ across a two-contact (photovoltaic or photochemical) device. The set of four rate equations for electron and hole partial currents, $J_n(x)$ and $J_p(x)$, at contacts x_1 and x_2[42], are given in **Figure 1**. The out-of-equilibrium surface-electron and -hole densities, $\Delta n = (n_x - n_x^{eq})$ and $\Delta p = (p_x - p_x^{eq})$, under illumination drive electron and hole partial currents. The magnitude of the current response is related directly to the kinetics of electron or hole transfer ($k_{1,et}$ or $k_{1,ht}$, and local species concentrations) or similarly the equilibrium exchange-current densities (J_{0n}^x and J_{0p}^x). These two equilibrium-exchange-current densities define the $(E_{fn} - E_{fp})/q$ and V_{oc} and therefore the maximum free energy available to do work under steady-state illumination. Interfacial kinetics places limits on the maximum "uphill" chemical reaction a photoabsorber can drive. *This kinetic model applies identically to photoabsorbers beyond bulk semiconductors, including particulate photocatalysts, and could be adapted to molecular absorbers.*

In particulate-semiconductor photoelectrochemistry, the above considerations *must simultaneously apply to two spatially separated contacts on the same light-absorbing particle*; one contact selectively collecting electrons and the other holes[43-45]. The carrier selectivity of these contacts, along with the inherent properties of the semiconductor (mobility, lifetime, absorption coefficient, etc.), determine the ability of the semiconductor to drive any given photochemical reaction with a specific ΔG_{rxn}. The measured "absolute" band-edge energies are of limited importance. Because many tests are done with sacrificial electron or hole acceptors (thus leading to a case where ΔG_{rxn} is near zero or even negative and spontaneous without light), understanding of the underlying physics has often been obscured.

Corrosion and Band-Edge Energies. Gerischer proposed that semiconductors are natively unstable in photoelectrochemical systems when the standard potentials for corrosion/decomposition are situated

within the band edges[46]. For example, the anodic reaction $CdS + 2h^+ \rightarrow Cd^{2+} + S$ has a standard potential more negative on an electrochemical scale than the valence band of CdS. As a result, *n*-CdS is thermodynamically unstable in water under illumination. However, this point does not mean that *n*-CdS and other semiconductors with similar energetics can't function meaningfully as photoelectrodes in water. The prolonged and stabilized operation of *n*-type CdS, ZnO, Cu_2O, CdTe, and metal dichalcogenide photoanodes in water has been achieved through manipulation of interfacial kinetics in two ways. One strategy is to alter the electrolyte chemistry so that the redox reactions of interest greatly outpace the undesirable corrosion reactions for the flux of photogenerated carriers. Kinetic strategies that speed the rate of productive reactions for electrons and holes through electrocatalysis will lower the steady-state population of electrons and holes at the surface (and quasi-Fermi-level splitting), also suppressing the competing corrosion reactions[47]. A second strategy is to coat the semiconductor surface with a protective thin film that specifically impedes corrosion/decomposition processes[48-50]. Such protective surface layers generally form a buried-junction-type structure where the charge-carrier selectivity of the passivating surface layer in contact with the bulk semiconductor controls the ability of the semiconductor to drive a specific reaction. We also note that because corrosion reactions take place on the semiconductor surface, and thus inside the EDL, their relative potentials shift in the same way as the band-edge potential if the semiconductor moves into inversion or accumulation – that is, corrosion reactions are not outer-sphere processes.

Summary. We clarify a common misconception of band-edge alignment with reduction potentials as a key material design principle for photocatalysts. Semiconductor absorbers can support excess charge densities where the kinetics of surface reactions will determine the resulting products. This clarification enables research of previously ignored materials and informs design principles for photocatalyst systems engineering for both one-electron redox reactions as well as for more complex multi-electron transfer reactions (e.g, H_2 evolution, H_2O oxidation, CO_2 reduction). In multi-electron transfer reactions, charge often accumulates at surface sites and how that charge is screened by electrolyte ions determines if the apparent band-edges shift with charge accumulation or not[15]. In the search for earth-abundant and efficient photocatalysts, the two primary materials parameters of importance are *i*) sufficient optoelectronic properties of the absorber (optical absorption coefficient and free-carrier lifetime) and *ii*) the ability to make both hole- and electron-carrier-selective contacts that serve to connect the semiconductor with catalytic sites that drive the oxidation and reduction half reactions of interest.

Acknowledgements. A.C.N. and S.W.B. are supported for this work through the Liquid Sunlight Alliance (DE-SC0021266), and G.J.M. through the Center for Hybrid Approaches in Solar Energy to Liquid Fuels (DE-SC0021173), both Energy Innovation Hubs funded by the U.S. Department of Energy, Office of Science, Office of Basic Energy Sciences. S.A. acknowledges support as part of Ensembles of Photosynthetic Nanoreactors (EPN), an Energy Frontier Research Center funded by the U.S. Department of Energy, Office of Science (DE-SC0023431). A.J.K acknowledges work funded by the Department of Energy, Basic Energy Sciences (award number DE-SC0014279). S.M. acknowledges support from the Department of Energy (award number DE-SC0006628).

References:

1 Li, J. & Wu, N. Semiconductor-based photocatalysts and photoelectrochemical cells for solar fuel generation: a review. *Cat. Sci. Tech.* **5**, 1360-1384, (2015).

2 Chen, S., Takata, T. & Domen, K. Particulate photocatalysts for overall water splitting. *Nat. Rev. Mater.* **2**, 17050, (2017).

3 Nozik, A. J. Photoelectrochemistry: Applications to solar energy conversion. *Annu. Rev. Phys. Chem.* **29**, 189-222, (1978).

4 Boettcher, S. W. *et al.* Photoelectrochemical hydrogen evolution using Si microwire arrays. *J. Am. Chem. Soc.* **133**, 1216-1219, (2011).

5 Weber, M. F. & Dignam, M. J. Efficiency of splitting water with semiconducting photoelectrodes. *J. Electrochem. Soc.* **131**, 1258-1265, (1984).

6 Marcus, R. A. Chemical and electrochemical electron-transfer theory. *Annu. Rev. Phys. Chem.* **15**, 155-196, (1964).

7 Marcus, R. A. & Sutin, N. Electron transfers in chemistry and biology. *Biochim. Biophys. Acta, Rev. Bioenerg.* **811**, 265-322, (1985).

8 Fajardo, A. M. & Lewis, N. S. Rate constants for charge transfer across semiconductor-liquid interfaces. *Science* **274**, 969-972, (1996).

9 Lewis, N. S. Chemical control of charge transfer and recombination at semiconductor photoelectrode surfaces. *Inorg. Chem.* **44**, 6900-6911, (2005).

10 Memming, R. in *Semiconductor Electrochemistry* 127-168 (Wiley-VCH 2015).

11 Moore, C. C. Ergodic theorem, ergodic theory, and statistical mechanics. *Proc. Natl. Acad. Sci.* **112**, 1907-1911, (2015).

12 Hisatomi, T., Kubota, J. & Domen, K. Recent advances in semiconductors for photocatalytic and photoelectrochemical water splitting. *Chem. Soc. Rev.* **43**, 7520-7535, (2014).

13 Ager, J. W., Shaner, M. R., Walczak, K. A., Sharp, I. D. & Ardo, S. Experimental demonstrations of spontaneous, solar-driven photoelectrochemical water splitting. *Energy Environ. Sci.* **8**, 2811-2824, (2015).

14 Chen, Z. *et al.* Accelerating materials development for photoelectrochemical hydrogen production: Standards for methods, definitions, and reporting protocols. *J. Mater. Res.* **25**, 3-16, (2010).

15 Laskowski, F. A. L., Nellist, M. R., Qiu, J. & Boettcher, S. W. Metal oxide/(oxy)hydroxide overlayers as hole collectors and oxygen-evolution catalysts on water-splitting photoanodes. *J. Am. Chem. Soc.* **141**, 1394-1405, (2019).

16 Lyon, L. A. & Hupp, J. T. Energetics of the nanocrystalline titanium dioxide/aqueous solution Interface: Approximate conduction band edge variations between $H_0 = -10$ and $H^- = +26$. *J. Phys. Chem. B* **103**, 4623-4628, (1999).

17 Lichterman, M. F. *et al.* Direct observation of the energetics at a semiconductor/liquid junction by operando X-ray photoelectron spectroscopy. *Energy & Environmental Science* **8**, 2409-2416, (2015).

18 Peper, J. L., Gentry, N. E., Boudy, B. & Mayer, J. M. Aqueous TiO_2 nanoparticles react by proton-coupled electron transfer. *Inorg. Chem.* **61**, 767-777, (2022).

19 Kautek, W. & Gerischer, H. Photoelectrochemical reactions and formation of inversion layers at n-type MoS_2, $MoSe_2$, and WSe_2 electrodes in aprotic solvents. *Ber. Bunsen-Ges. Phys. Chem.* **84**, 645-653, (1980).

20 Jaeger, C. D., Gerischer, H. & Kautek, W. Formation of an inversion layer in n-type $MoSe_2$ electrodes: Observation in the presence of highly oxidizing redox systems. *Ber. Bunsen-Ges. Phys. Chem.* **86**, 20-25, (1982).

21 Royea, W. J., Michalak, D. J. & Lewis, N. S. Role of inversion layer formation in producing low effective surface recombination velocities at Si/liquid contacts. *Appl. Phys. Lett.* **77**, 2566-2568, (2000).
22 Grimm, R. L. *et al.* Comparison of the photoelectrochemical behavior of H-terminated and methyl-terminated Si(111) surfaces in contact with a series of one-electron, outer-sphere redox couples in CH_3CN. *J. Phys. Chem. C* **116**, 23569-23576, (2012).
23 Gstrein, F., Michalak, D. J., Knapp, D. W. & Lewis, N. S. Near-surface channel impedance measurements, open-circuit impedance spectra, and differential capacitance vs potential measurements of the Fermi level position at Si/CH_3CN contacts. *J. Phys. Chem. C* **111**, 8120-8127, (2007).
24 Park, K.-W. & Kolpak, A. M. Optimal methodology for explicit solvation prediction of band edges of transition metal oxide photocatalysts. *Commun Chem* **2**, 1-10, (2019).
25 Trasatti, S. The absolute electrode potential: an explanatory note *Pure Appl. Chem.* **58**, 955-966, (1986).
26 Sze, S. M. & Ng, K. K. *Physics of semiconductor devices*. (John Wiley & Sons, Inc., 2006).
27 Michalak, D. J. & Lewis, N. S. Use of near-surface channel conductance and differential capacitance versus potential measurements to correlate inversion layer formation with low effective surface recombination velocities at *n*-Si/liquid contacts. *Appl. Phys. Lett.* **80**, 4458-4460, (2002).
28 Turner, J. A., Manassen, J. & Nozik, A. J. Photoelectrochemistry with *p*-Si electrodes: Effects of inversion. *Appl. Phys. Lett.* **37**, 488-491, (1980).
29 Keller, N. D. *et al.* Multi-electron transfer at H-terminated p-Si electrolyte interfaces: Large photovoltages under inversion conditions. *J. Am. Chem. Soc.* **145**, 11282-11292, (2023).
30 Bard, A. J., Bocarsly, A. B., Fan, F. R. F., Walton, E. G. & Wrighton, M. S. The concept of Fermi level pinning at semiconductor/liquid junctions. Consequences for energy conversion efficiency and selection of useful solution redox couples in solar devices. *J. Am. Chem. Soc.* **102**, 3671-3677, (1980).
31 Bocarsly, A. B., Bookbinder, D. C., Dominey, R. N., Lewis, N. S. & Wrighton, M. S. Photoreduction at illuminated p-type semiconducting silicon photoelectrodes. Evidence for Fermi level pinning. *J. Am. Chem. Soc.* **102**, 3683-3688, (1980).
32 Spitler, M. T. Impedance analysis of semiconductor electrodes in the accumulation region. *Sustain. Energy Fuels*, (2023).
33 Hofstein, S. R. & Warfield, G. Physical limitations on the frequency response of a semiconductor surface inversion layer. *Solid-State Electron.* **8**, 321-341, (1965).
34 Madou, M. J., Loo, B. H., Frese, K. W. & Morrison, S. R. Bulk and surface characterization of the silicon electrode. *Surf. Sci.* **108**, 135-152, (1981).
35 Cooper, G., Turner, J. A. & Nozik, A. J. Mott-Schottky plots and flatband potentials for single crystal rutile electrodes. *J. Electrochem. Soc.* **129**, 1973-1977, (1982).
36 Thapar, R. & Rajeshwar, K. Mott—Schottky analyses on n- and p-GaAs/room temperature chloroaluminate molten-salt interfaces. *Electrochim. Acta* **28**, 195-198, (1983).
37 Bardwell, J. A., Draper, N. & Schmuki, P. Growth and characterization of anodic oxides on Si(100) formed in 0.1 M hydrochloric acid. *J. Appl. Phys.* **79**, 8761-8769, (1996).
38 Huygens, I. M. & Strubbe, K. Electrochemical impedance study of the germanium/electrolyte interface. *J. Electrochem. Soc.* **155**, F49, (2008).
39 La Mantia, F., Habazaki, H., Santamaria, M. & Di Quarto, F. A critical assessment of the Mott-Schottky analysis for the characterisation of passive film-electrolyte junctions. *Russ. J. Electrochem.* **46**, 1306-1322, (2010).

40 Molto, C., Etcheberry, A., Grand, P. P. & Goncalves, A. M. Study of photo-oxidized n-type textured silicon surface through electrochemical impedance spectroscopy. *J. Electrochem. Soc.* **167**, 146505, (2020).
41 Würfel, P. & Würfel, U. *Physics of solar cells: from basic principles to advanced concepts*. 3rd edition edn, (Wiley-VCH, 2016).
42 Roe, E. T., Egelhofer, K. E. & Lonergan, M. C. Limits of contact selectivity/recombination on the open-circuit voltage of a photovoltaic. *ACS Appl. Energy Mater.* **1**, 1037-1046, (2018).
43 Pan, Z. *et al.* Elucidating charge separation in particulate photocatalysts using nearly intrinsic semiconductors with small asymmetric band bending. *Sustain. Energy Fuels* **3**, 850-864, (2019).
44 Pan, Z. *et al.* Mutually-dependent kinetics and energetics of photocatalyst/co-catalyst/two-redox liquid junctions. *Energy Environ. Sci.* **13**, 162-173, (2020).
45 Liu, T. *et al.* A general interfacial-energetics-tuning strategy for enhanced artificial photosynthesis. *Nat. Commun.* **13**, 7783, (2022).
46 Gerischer, H. On the stability of semiconductor electrodes against photodecomposition. *J. Electroanal. Chem. Interf. Electrochem.* **82**, 133-143, (1977).
47 Yu, W. Understanding the stability of semiconducting photocathodes for solar water splitting. *Curr. Opin. Electrochem.* **39**, 101262, (2023).
48 Zhao, T. *et al.* A coating strategy to achieve effective local charge separation for photocatalytic coevolution. *Proc. Natl. Acad. Sci.* **118**, e2023552118, (2021).
49 Shen, X. *et al.* Tuning intermediate bands of protective coatings to reach the bulk-recombination limit of stable water-oxidation GaP photoanodes. *Adv. Energy Mater.* **12**, 2201314, (2022).
50 Shen, X. *et al.* Comprehensive evaluation for protective coatings: Optical, electrical, photoelectrochemical, and spectroscopic characterizations. *Front. Energy Res.* **9**, (2022).